AIAA 80-0189R

Multiple-Tactical Aircraft Combat Performance Evaluation System

D.S. Hague*
Aerophysics Research Corporation, Bellevue, Wash.

The multiple-tactical aircraft combat performance evaluation system (MULTAC) is designed to analyze the outcome of a close-in M-on-N air battle involving up to 20 aircraft and their associated weapons. Construction of MULTAC including target selection, guidance and control laws, weapon system modeling, and other aspects involved in the computation of up to 20 simultaneous reacting aircraft flight paths are discussed. Encounter outcome is rated by the average survival probability of each aircraft force. Either a cokill probability model or a Monte-Carlo model may be employed in this evaluation. Typical results emphasizing the difference between one-on-one and M-on-N encounters are presented. These results illustrate the tradeoff between advanced technology and number of aircraft in aerial combat encounters. Construction of the MULTAC system provides fighter designers with a tool for evaluating the impact of advanced technology items on aerial combat performance at the preliminary design level.

System Outline

THE multiple-tactical aircraft combat performance evaluation system (MULTAC) is illustrated in schematic fashion in Fig. 1. The trajectories of up to 20 aircraft engaged in an aerial combat encounter are simultaneously integrated using the fourth-order Runge-Kutta algorithm. These trajectories are integrated under time-varying angle of attack, bank angle, and throttle history control. Appropriate control histories are developed by a combat tactics logic which combines the target selection, control law specification, single-shot kill probability P_k computation, and firing opportunity selection functions.

Encounter outcome may be determined by a "sudden death" model in which aircraft are removed from the encounter on the basis of single-shot P_k and the application of a random chance mechanism. Using this approach an encounter must be repetitively simulated using Monte-Carlo methods to determine the average result. Such an approach provides an estimate of both the mean result and the associated scatter about the mean. An alternate approach, the cokill probability model,[1] develops an approximation to the mean result on the basis of a single-encounter simulation.

Generally the computation of optimal mini-max solutions to an aerial combat engagement must be limited to far more simplified dynamic models of aerial combat than the one considered here. For example, the constant-speed planar games of Ref. 2 yield to mini-max solution by application of Isaacs' differential game theory.[3] However, computation of differential game solutions for many aircraft using realistic three-dimensional dynamics is computationally infeasible by current methodology and equipment. An alternative approach is to fix the control laws of one side in the encounter and then to determine the optimal response of the second force in response to the tactics of the first force.

This approach has a certain intuitive appeal for it closely parallels the evolution of "optimal" tactics in aerial warfare where historically one side will find a combat tactic which leads to a temporary advantage. The second side will then develop a response by trial-and-error methods which effectively nullifies the advantage of the first side. In this sense when studying aerial combat we are not dealing with the stationary system that results from the differential game methodology.

There are at least two fundamental approaches to the determination of an optimal response to fixed tactics by one force. The first method is to apply the variational calculus: for example, Ref. 4 applies an extension of Bryson and Denham's[5] variational steepest descent algorithm to this problem. The second approach is to parameterize the controls of the force to be optimized and to apply the methods of multivariable search[6,7] to determine an optimal response to fixed tactics. This latter approach is the one employed in MULTAC.

In applying MULTAC to the analysis of M-on-N aerial combat, it is convenient to have a library of tactical aircraft and weapon characteristics available. Such a library, encompassing current United States and Soviet tactical aircraft forms part of the MULTAC system. These characteristics are stored in an on-line computerized data base.

Interpretation of M-on-N encounter results involving multiple interacting trajectories requires the application of modern computer graphics equipment. To aid in such an interpretation, both *storage tube* devices (such as the widely distributed Tektronix terminals) and *refresh graphics* devices are used to illustrate an encounter from the viewpoint of an external observer, or alternatively the cockpit view from any of the aircraft in the engagement may be presented. With storage tube devices, a series of still pictures is presented in chronological order. With the refresh graphics devices a moving picture of the encounter is generated at a rate approaching that of real time.

Planetary and Vehicle Characteristics

A spherical nonrotating planetary model is employed in the MULTAC system. The spherical planet is used (rather than the usual flat Earth model employed in most one-on-one aerial combat engagement models) in order to facilitate the introduction of radar-imaging models for ground-based radars. An inverse square gravitational field and a two-layer approximation to the 1962 U.S. Standard Atmosphere, accurate up to 65,600 ft, completes the MULTAC planetary model. (Extension to cover aerial combat at altitudes to 106,700 ft would require addition of the third layer of the U.S. Standard Atmosphere.[8])

Vehicle characteristics modeled in MULTAC consist of exterior geometry, aerodynamic forces, propulsive forces, and fuel flows. The standard library of vehicles available to

Received Jan. 9, 1980; presented as Paper 80-0189 at the AIAA 18th Aerospace Sciences Meeting, Pasadena, Calif., Jan. 14-16, 1980; revision received Aug. 27, 1980. This paper is declared a work of the U.S. Government and therefore is in the public domain.

*President. Member AIAA.

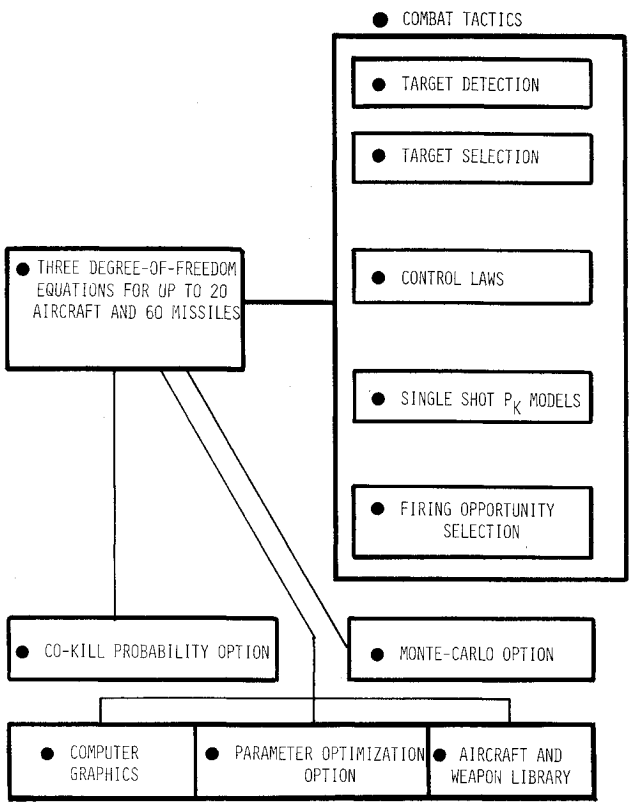

Fig. 1 Schematic of MULTAC system.

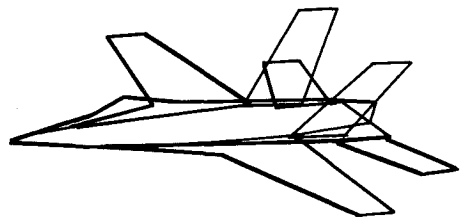

Fig. 2 Computer graphics F-18 model.

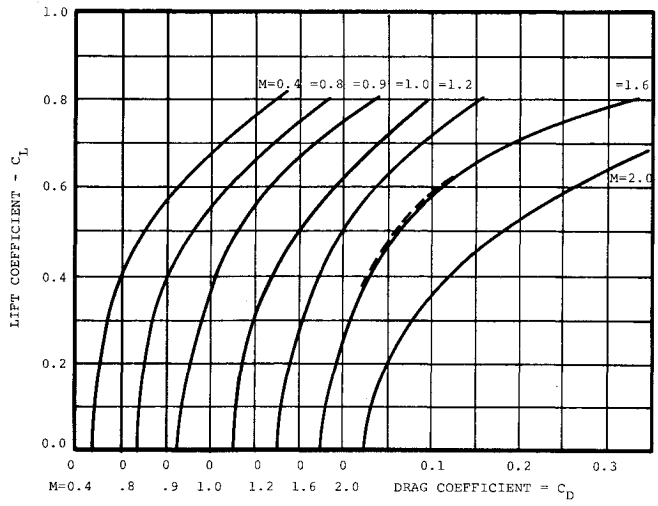

Fig. 3 Accuracy of fourth-order polynomial, C_L vs C_D.

the system consists of the F-4E Phantom, F-5E Tiger II, F-15 Eagle, F-16 lightweight fighter, F-18 Hornet, MIG-21 Fishbed, MIG-23 Flogger, and MIG-25 Foxbat. Additional aircraft types may be readily added to this data base.

Aircraft geometries are represented by straightforward line drawings which provide trajectory and cockpit displays. A typical line drawing at the level used in MULTAC computer graphic displays is presented in Fig. 2.

Aerodynamic characteristics consist primarily of nonlinear lift curves and drag polars to high angles of attack. Previous air combat models, e.g., Ref. 9, have tended to use detailed aerodynamic data from the appropriate aircraft Performance Handbook (typified by Ref. 10). Such data have been stored at discrete points, and standard interpolation techniques have been employed to predict lift and drag as functions of angle of attack and Mach number.

A more compact data storage technique is employed in MULTAC. Here fourth-order polynomials are used to curve fit lift curves and drag polars at constant Mach number:

$$C_L(\alpha;M) = a_0 + a_1\alpha + a_2\alpha^2 + a_3\alpha^3 + a_4\alpha^4 \qquad (1)$$

$$C_D(C_L;M) = b_0 + b_1C_L + b_2C_L^2 + b_3C_L^3 + b_4C_L^4 \qquad (2)$$

Lift and drag at intermediate Mach numbers can be found by interpolation using the constant Mach number results from Eqs. (1) and (2). Thus only the Mach-number-dependent polynomial coefficients a_i and b_j need be stored in the MULTAC system. Accuracy of these models is illustrated in Fig. 3. Here MIG-21 drag polars predicted by Axelson's method[11] are compared to the polynomial approximations at Mach numbers up to 2.0. Only at $M=1.6$ is any difference apparent between theoretical drag polars and polynomial approximation.

A similar polynomial approximation is used to represent propulsive characteristics. Thrust and fuel flows at constant altitude are modeled as fourth-order polynomials in Mach number

$$T(M;h) = C_0 + C_1M + C_2M^2 + C_3M^3 + C_4M^4 \qquad (3)$$

$$\dot{W}(M;h) = d_0 + d_1M + d_2M^2 + d_3M^3 + d_4M^4 \qquad (4)$$

and characteristics at intermediate altitudes are determined by interpolation.

Other vehicle characteristics required in the course of an aerial combat engagement analysis include cockpit limits of visibility; radar characteristics; weapon number, types, and single-shot kill probabilities; maximum angle of attack as a function of Mach number; vehicle load factor limits; pilot tolerance to acceleration; and available fuel loads.

Equations of Motion

Equations of motion employed in MULTAC describe the three degrees-of-freedom motion for up to 20 aircraft engaged in interactive combat trajectories. These equations are of the form

$$\{\dot{x}_{ij}(t)\} = \{f(x_{ij}(t), \alpha_{kj}(t), t)\} \qquad i=1,2,\ldots,7$$

$$j=1,2,\ldots,N_A \qquad k=1,2,3 \qquad (5)$$

Here, N_A is the number of aircraft, the suffix i indicating the state component number and the suffix j the aircraft number. Thus, the state components (1, j), (2, j), and (3, j) are the positional state components for three-dimensional flight. State components (4, j), (5, j), and (6, j) are the velocity components of state, and the state components (7, j) are the vehicle masses.

The three control variable vector components $\alpha_{kj}(t)$ represent angle of attack, bank angle, and throttle, respectively. Where thrust vector control is available, thrust deflection is also a control vector component. Other possible control variables for advanced tactical aircraft include direct aerodynamic force controls and steerable gun angles. In the MULTAC simulation all components of the control vector are subject to limiting rates, that is

$$\left\{\left|\frac{d\alpha}{dt}\right| \le R\right\} \qquad (6)$$

where R is the vector of control rate limits.

Propulsive forces are computed in aircraft body axes and then transferred to the local wind axes and combined with aerodynamic forces. The propulsive and aerodynamic force vector is then transformed into local geocentric coordinates and combined with gravitational force. The total propulsive, aerodynamic, and gravitational force vector is then transformed into a rectangular Earth-centered system and integrated using the fourth-order Runge-Kutta algorithm.

Using this system the trajectories of 20 interacting aircraft are determined by integrating 140 coupled nonlinear ordinary differential equations under the influence of 60 basic control variables. This integration may impose a significant burden on available computational equipment when either Monte-Carlo or optimization studies are conducted.

Equations of motion are integrated forward in time from a given initial state

$$\{x_{ij}(0)\} = \{x_{0_{ij}}\} \tag{7}$$

Instantaneous control vector values are determined on the basis of vehicle relative states and the combat tactics of the next section subject to the rate limits of Eq. (6).

Combat Tactics

Combat tactics encompass the targeting, control determination, P_k computation, and weapon firing selection logic functions. Each of these functions is described below.

Targeting

The targeting problem consists of determining the appropriate sequence of opposing aircraft as a function of time throughout the encounter. Generally, this decision is based on the relative state of a given aircraft and that of all possible opponents. If the aircraft of one force are practicing coordinated tactics, then target selection also includes consideration of the friendly aircraft states in the decision-making process. Where incomplete information is available to an aircraft, then only a restricted number of opposing vehicle state components are known. These restrictions may include total ignorance of the presence of some subset of the opposing force's aircraft. It is assumed that the fuel state of the opposing aircraft cannot be known.

Two limiting cases are of some interest in aerial combat encounters. These are the uncooperative pilot who is aware of aircraft only in his sensor or visual fields of view, and the fully aware pilot who by virtue of a high degree of cooperation with his fellow pilots is able to catalog the current state of all opponents.

Targeting decisions in the MULTAC system are largely based on conditions in the angle-off/steering error plane. Angle-off is the angle between the line-of-sight vector connecting an aircraft to a given opponent and that opponent's velocity vector. Steering error is the cone angle between an aircraft's velocity vector and a given opponent's position. During an actual aerial combat engagement *steering error* to observable opponents is readily assessed. *Angle-off* is more difficult to observe directly due to visual or sensor limitations; however, the experienced pilot may employ other visual motion cues to aid in an assessment of this latter quantity.

The angle-off/steering error or targeting plane is illustrated in schematic fashion in Fig. 4. At the origin (0, 0) an aircraft sits on its opponent's tail. At the diagonally opposite corner (180, 180) an aircraft finds the situation reversed, and an opponent has achieved a tail attack position. Along the principle diagonal connecting (0, 180) and (180, 0) a series of positions providing *angular equality* are encountered. These positions vary from flying apart to parallel or antiparallel flight to head-on attacks. The principle diagonal is the locus of *actual* equality when equal aircraft enjoying equal states encounter each other. Otherwise, actual equality is also a function of aircraft states and performance capability.

An aircraft maneuvering to draw its opponent away from the diagonal toward the origin places that opponent at a disadvantage. The degree of disadvantage can be measured by distance d from the diagonal. Conversely, as an opponent succeeds in maneuvering an aircraft toward the opposite corner at (180, 180) the aircraft becomes increasingly disadvantaged.

At each time point the MULTAC targeting algorithm computes the distance of each opponent from the diagonal assigning a positive value to distance in the favorable lower left half-plane and negative values to the unfavorable upper right half-plane. A value judgment is then made: whether to attack the most disadvantaged opponent or to defend from the most advantaged opponent. That is, the opponent is selected by examining the functions

$$d^{(+)} = \max[d_i]; i = 1,2,\ldots,N_O \tag{8}$$

where N_O is the number of observed opponents or the function

$$d^{(-)} = \min[d_i]; i = 1,2,\ldots,N_O \tag{9}$$

In the simplest case this judgment can be made on the basis of the function

$$\phi = \operatorname{sgn}[d^{(+)} + d^{(-)}] \tag{10}$$

More generally, a bias toward attack or defense can be introduced by switching from attack to defense on the basis of the quadratic form function

$$\phi = \operatorname{sgn}\left([d^{(+)}, d^{(-)}]\begin{bmatrix} w_{11} & w_{12} \\ w_{21} & w_{22} \end{bmatrix}\begin{Bmatrix} d^{(+)} \\ d^{(-)} \end{Bmatrix}\right) \tag{11}$$

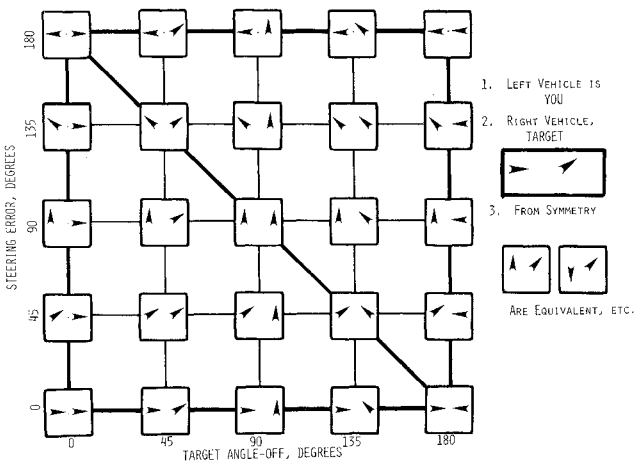

Fig. 4 Angular rating in angle-off/steering error plane.

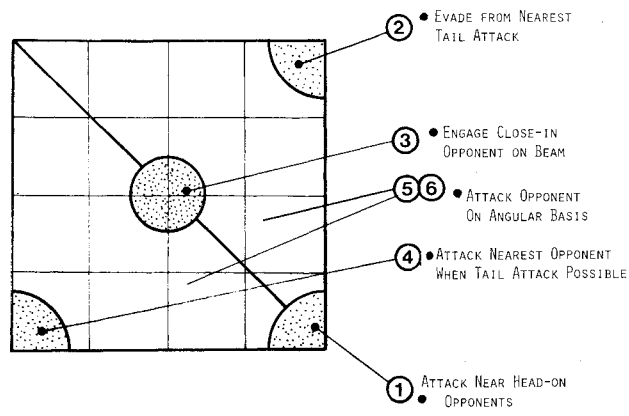

Fig. 5 Primary target selection mode.

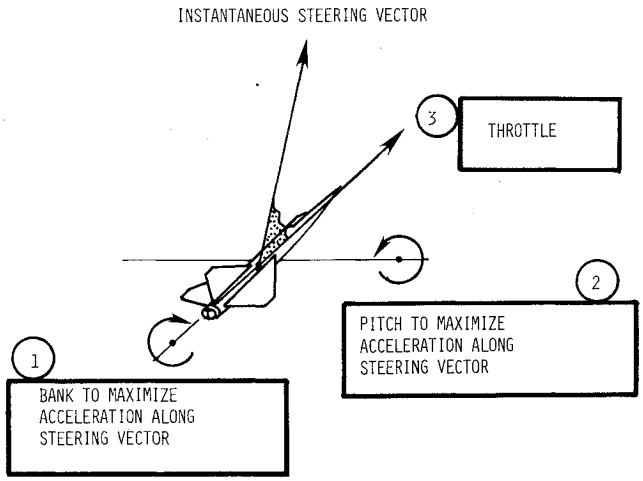

Fig. 6 Basic steering vector and control variables.

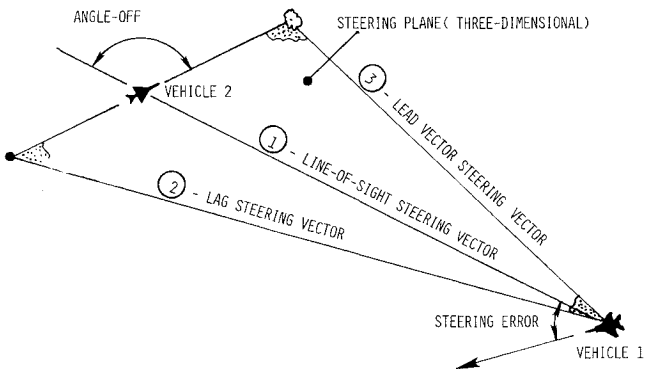

Fig. 7 Steering vector options.

More complex targeting algorithms also account for other relative state components. Figure 5 illustrates some preferential targeting states which may be introduced. These include

Region 1: Near head-on opponents—attack the nearest.

Region 2: Opponents attacking from the rear—evade from the nearest.

Region 3: Close-in opponent flying nearly parallel on the beam—such opponents may prevent a sustained tail attack on region 4.

Region 4: Opponent's presenting a tail aspect position—attack the nearest.

Regions 5 and 6 use Eq. (11) for target selection.

MULTAC also recognizes the target fixation problem by providing a minimum time between switching targets. Combat experience also dictates that a maximum period of time be assigned to any one target on the assumption that an unobserved opponent may be taking advantage of an aircraft which maneuvers against any one opponent for too long a period.

Combat Guidance

Combat guidance laws are used to define instantaneous commanded values for the trajectory controlling variables discussed previously. MULTAC primarily bases the commanded values on the position of the target vehicle in the angle-off/steering error plane of Fig. 4. Given the target vehicle's angular position and the relative vehicle states, a steering vector is defined (Fig. 6). An aircraft banks to place this steering vector on the canopy centerline and simultaneously pitches to maximize the acceleration along this vector subject to the following constraints: 1) instantaneous maximum angle of attack, 2) aircraft and pilot load factor limits, and 3) specific energy considerations.

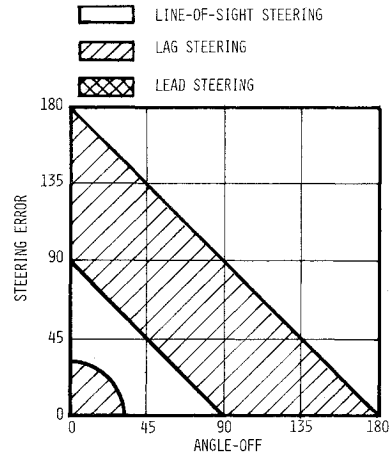

Fig. 8 Tail attack steering law, the lag "bucket."

Various steering vector definitions may be employed in MULTAC. The steering vector is defined relative to the plane containing an aircraft's position and the target vehicle's velocity (Fig. 7). In the simplest case the line of sight connecting the two aircraft may be employed as the steering vector. Another steering vector of interest is the lead-pursuit vector. In MULTAC this vector is the path which would produce a collision between a fired missile and the target if the target continued in unaccelerated flight. Another vector of interest is the lag-pursuit vector which results in an aircraft attempting to steer into the rear of the target aircraft. A single parameter ϵ varying in the range $(+1, 0, -1)$ can be used to produce a range of steering vectors varying from lead to line of sight to lag pursuit.

Several steering vector selection algorithms are available in MULTAC. The most straightforward option is to place an opponent on the canopy centerline throughout the encounter; that is, to fly continuously using line-of-sight steering vectors to the sequence of selected opponents. Maneuvers of this type tend to lead to "scissoring" attacks with firing opportunities occurring at high angles-off.[12]

If tail attack positions are sought, the sequence of the lag, line-of-sight, and lead steering vectors of Fig. 8 may be employed. Here a steering vector is selected on the basis of the target aircraft's position in the steering error/angle-off plane. Against a target in the disadvantaged upper right half-plane, line-of-sight steering is practiced. Thus, when an aircraft is disadvantaged in an angular sense, the decision is made to pull hard against the opponent of the moment in an attempt to improve angular position. If this type of maneuver is successful in improving angular position and the principle diagonal is crossed so that an aircraft obtains the angular advantage, then the line-of-sight vector is replaced by a lag steering vector. At this point an aircraft is attempting to convert angular to positional advantage and seeks to attain a position to the rear of an opponent. Success of this tactic depends on both the relative states and the physical characteristics of the aircraft and its target. It is possible that reverting to lag steering will result in the target regaining the angular advantage, for by symmetry the target is in the disadvantaged half-plane and pulling hard to the line-of-sight vector.

When the combination of relative state and vehicle characteristics permits an aircraft to continue to improve angular position while employing lag steering, the target may be forced across the 90 deg line of advantage midway between the origin and principle diagonal in the angle-off/steering error plane. Should this occur, an aircraft reverts to line-of-sight steering in an attempt to convert to a firing position from the target's rear quadrant. Finally, when a position within 30 deg of the tail attack position is achieved, then a lead steering vector based on relative state and weapon

characteristics is employed. When the angle between an aircraft's body axis and the lead steering vector is less than the allowable steering error for weapon firing, the advantaged aircraft reduces its normal load factor, and weapon firing is permitted.

It should be noted that converting to a tail attack position can and usually does require a significantly greater time than that of the high angle-off "slashing" attacks produced by line-of-sight steering. In the one-on-one encounter the time required for a tail attack may be available. In the larger scale M-on-N encounter the longer duration tail attack maneuver may result in an unacceptable period of target fixation in view of the presence of multiple aircraft threats.

Single-Shot Kill Probabilities

Single-shot kill probability models are used to determine the effectiveness of a weapon firing opportunity. These models compute weapon effectiveness as an isolated event, that is, it is assumed that both the attacking aircraft and the target aircraft have 100% survival probability prior to the firing. Single-shot kill probabilities for the major United States and Soviet air-to-air missiles are available for use in MULTAC. Typically, these models determine when weapon firing constraints are satisfied, determine weapon flight time to target, and the probability of kill.

Weapon firing constraints typically consist of minimum and maximum range together with the allowable steering error and target angle-off at launch. Weapon flight times are based on a closing of the lead pursuit triangle using aircraft and weapon characteristics. For semiactive missiles, which depend on the return of reflected electromagnetic energy from the target, the weapon flight time is used to determine the period in which a target must remain illuminated by the attacking aircraft.

Kill probability is usually a stored function of target aspect at the moment of launch. This probability includes the combined probabilities of successful launch and release from the carrying rail, acquisition and retention of guidance, fuzing success, and kill probability of the destructive mechanism given a successful hit.

Weapon Firing

MULTAC permits either the individual firing or a rapid fire "rippling-off" mode of weapon disposal at a given firing opportunity. Generally in an aerial combat encounter of significant duration, many firing opportunities arise but only a limited number of weapons are carried. The firing logic employed does require a specified time interval between successive weapon firings in either the ripple or single-shot modes. Nevertheless, an excess of opportunities over the weapon number carried is frequently encountered in combat simulations.

Now to a given firing policy of the blue force, the red force can adopt one of several firing policy options. The resulting encounter ratings will vary with the firing policies of both blue and red forces, and these ratings can therefore be arranged in the form of an ordinary game matrix.[13] These game matrices are readily generated by MULTAC. Determination of the optimal firing policy combination can be made by applying standard game theory methods and may involve practicing a mixed strategy.

In studies to date it has been found that a near optimal policy is for both sides to fire their weapons singly at the first N_W opportunities. Here N_W is the number of weapons carried by an aircraft. The advantage of utilizing early firing opportunities, even though these may not offer the highest single-shot P_k, is that they reduce the probability of the target's succeeding firings.

Rating the Encounter

Sudden-Death Model—Monte-Carlo Method

When a weapon firing occurs in actual combat an aircraft is destroyed, or survives, on the basis of the associated single-shot P_k. Force attrition associated with this process can readily be modeled. At each firing opportunity the probability of survival is

		RED SURVIVAL					Σ
		0	1	2	3	4	
BLUE SURVIVAL	0	0	2	1	0	0	3
	1	3	7	5	3	1	19
	2	4	18	14	6	2	44
	3	0	11	7	4	0	22
	4	0	10	1	1	0	12
	Σ	7	48	28	14	3	

Fig. 9 Typical scatter obtained in Monte-Carlo analysis.

$$Q_i = \begin{cases} 0; M_i \le P_{k_i} \\ 1; M_i > P_{k_i} \end{cases} \tag{12}$$

Here Q_i is the target survival probability at the ith shot, P_{k_i} the single-shot kill probability of this shot, and M_i a uniform random number generated in the interval 0-1. Thus as the trajectory equations are integrated in time, firing opportunities occur and weapons are fired. As the sequence of firings occurs, the target aircraft survive or are destroyed on the basis of Eq. (12). A destroyed aircraft is eliminated from the encounter, otherwise the target aircraft is unharmed and continues as an active participant.

It must be noted that in actual combat, or in combat simulation using this approach, the outcome is only one sample of a random process driven by the stochastic nature of current weapon kill mechanisms. When aircraft meet in an M-on-N encounter there are precisely $(M+1)\cdot(N+1)$ possible outcomes for we can have (0,1,2,...M) survivors on one side and (0,1,2...N) survivors on the other side. None of these $(M+1)\cdot(N+1)$ discrete outcomes is likely to provide a reasonable estimate of the mean survival probabilities of the forces involved. Figure 9 illustrates this point. Here a four-on-four encounter is simulated 100 times and the frequency with which each possible force survival combination occurs is recorded in a matrix of outcomes. For example, in these repetitive simulations three blue and two red aircraft survived 7% of the time. The most frequently observed result is two blue and one red survivors which occurred 18% of the time. Adding the matrix rows we obtain the frequencies with which an observer stationed at the blue force home base would record none through four survivors returning. Adding the columns gives the corresponding survival probabilities for red. The most frequent number of blue survivors is two, the most frequent number of red survivors is one. Average survival probabilities for aircraft in each force can be found by adding the total number of aircraft which return to base and dividing by the totals leaving base.

$$\bar{Q}_B = \frac{\sum_{i=1}^{N_B} (if_i)}{100N_B} \quad \text{and} \quad \bar{Q}_R = \frac{\sum_{j=1}^{N_R} (jf_j)}{100N_R} \tag{13}$$

Here $\bar{Q}_B$ and $\bar{Q}_R$ are the average survival probabilities for aircraft in the blue and red forces, f_i and f_j the frequencies with which i blue and j red survivors are recorded, N_B and N_R

the number of blue and red aircraft in each of the encounters, respectively. Evaluating Eq. (13) over the encounters of Fig. 9 we obtain $\bar{Q}_B = 55.25\%$ and $\bar{Q}_R = 39.5\%$, a significant advantage in favor of blue. Note that the average result is not one of the 25 distinct results obtained from the encounters.

It is interesting to examine these results in terms of the exchange ratio, here defined to be the number of red aircraft lost per blue loss.

$$X = \left(\frac{1-\bar{Q}_R}{1-\bar{Q}_B}\right) = 1.352$$

Examining the matrix of Fig. 9 the most frequent result, two blue and one red survivors, produces an exchange ratio of 1.50. The closest estimate of surviving aircraft possible which can be made from the discrete cases in the matrix is two blue and two red survivors. This result is 5.25% low for blue and 10.5% high for red. However, this result produces an exchange ratio of only 1.00.

Despite the overall superiority of blue in these encounters, red manages to achieve a draw 25% of the time. These results occur on the principle diagonal of Fig. 9. More surprisingly red wins, which are recorded above this diagonal, occur 20% of the time.

The scatter of Fig. 9 is solely due to weapon stochastic kill mechanisms. In the encounters studied weapons had an average P_k of 0.3 and all-aspect capability. The aircraft flown were F-4E Phantoms, however the blue aircraft were modified to provide 25% additional lift at all angles of attack. Clearly the scatter observed precludes the prediction of average encounter result on the basis of a single encounter. A single sample has a 20% chance of predicting a win for the overall losing side or a 25% chance of predicting a draw when in actuality the winning blue side destroys 35% more red aircraft than it loses over 100 encounters. Results of this type become of considerable significance when attempts are made to establish aircraft relative combat capability from a limited number of flight tests or simulations. It is also clear that in actual aerial warfare many engagements may occur before a definitive ranking of opposing aircraft types can be accomplished.

Cokill Probability Model

The cokill probability model for rating M-on-N aerial combat was introduced in Ref. 1. Instead of emulating aerial combat by eliminating aircraft at weapon firings in accordance with Eq. (12), with this model we retain all aircraft in the encounter but vary their probabilities of survival. In this way we seek to predict average survival probabilities by a single simulation of the encounter. At any instant in time during the encounter let two aircraft have survival probabilities $Q_i(t)$ and $Q_j(t)$ and suppose that aircraft i fires at aircraft j at this instant.

$$\Delta P_{ij}(t) = Q_i(t) Q_j(t) S_{ij}(t) \tag{14}$$

where $S_{ij}(t)$ is the single-shot P_k discussed previously. At some future instant in time

$$Q_j(t+\Delta t) = Q_j(t) - \Delta P_{ij}(t)$$

$$= Q_j(t)\,[1 - Q_i(t) S_{ij}(t)] \tag{15}$$

Equations (14) and (15) are the cokill probability difference equations which must be integrated together with the trajectory differential equations [Eq. (5)]. Thus, a single integration of Eqs. (5), (14), and (15) provides an approximate estimate of the mean result over many encounters.

The cokill model may also be extended to incorporate a cumulative damage model which reflects the combined effect of multiple shots on an aircraft. In its simplest form this extension is made by eliminating an aircraft when its survival probability falls below some specified value, say 20%.

Optimization

Optimization capability in MULTAC is currently limited to application of multivariable search techniques to the guidance parameters of one side or the other. Typical parameters which may be varied in this manner include initial states, targeting algorithms, and control laws. In the simplest case the best set of maximum load factors or angles of attack may be determined over a specified engagement. In a more complex situation the best positions for the lag steering corridor of Fig. 8 may be determined.

Payoff functions available include exchange ratio, red survival probability, and blue survival probability. Thus blue might seek to maximize exchange ratio or blue survival probability or to minimize red survival probability. References 6 and 7 describe multivariable search techniques suitable for aerial combat application. All these methods employ systematic parameter perturbations to establish directions in the free-parameter N space which efficiently improve the selected payoff criterion. Here N is the number of free parameters in the problem specification. These directions are exploited by subsequent one-dimensional searches along their corresponding vectors.

It should be noted that the payoff functions of aerial combat are discontinuous in the free-parameter space for firing opportunities occur at discrete time intervals. A small trajectory change may not establish an additional firing opportunity or eliminate an existing one. In this case only the single-shot kill probabilities, which are slowly changing functions of relative state, will be affected. A large perturbation may introduce or eliminate firing opportunities and at the point where the number of opportunities changes the payoff function will exhibit a discontinuity in parameter space. Little has been written on the optimization of discontinuous functions; however, this topic is briefly treated in Ref. 6. At the present time it should be noted that methods which depend on the existence of derivatives may fail to determine reasonable directions to follow in the neighborhood of these discontinuities. This behavior emphasizes the use of methods which do not require derivatives. This latter class of search includes methods using one parameter at a time and the accelerated random walk techniques of Ref. 6.

Advanced Technology Tradeoff Example

Consider a series of encounters between a red force equipped with F-4E Phantoms and a blue force equipped with modified versions of this aircraft. Let the modification produce a 25% lift increment at a given angle of attack throughout the flight envelope with no increase in drag force.

Now consider a series of engagements between the two forces with red initially flying to the north and blue positioned 4 n.mi. to the west at maneuver commencement. Let all aircraft be initially flying at Mach 0.9 and 20,000 ft. For reference purposes first examine the case in which both red

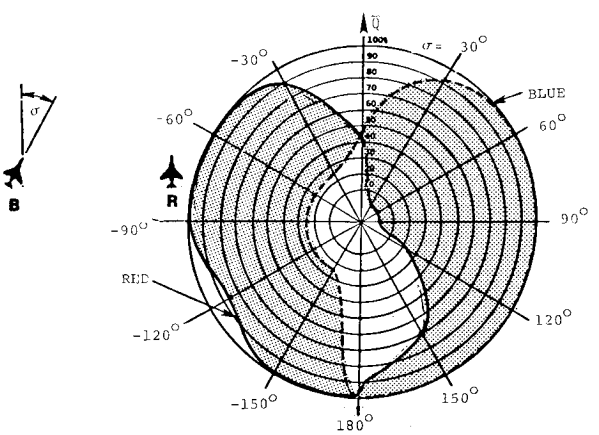

Fig. 10 One-on-one survival probability, equal aircraft.

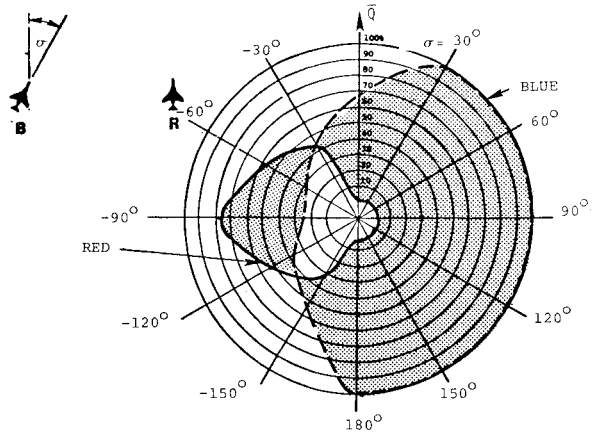

Fig. 11 One-on-one survival probability, advanced blue aircraft.

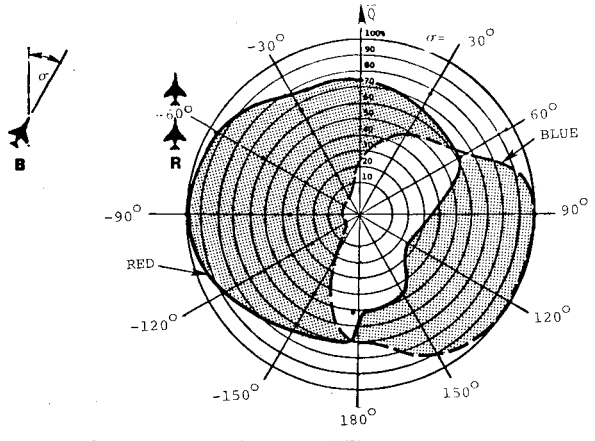

Fig. 12 One-on-two survival probability, advanced blue aircraft.

and blue fly standard F-4E aircraft and meet in one-on-one combat. Figure 10 illustrates predicted survival probabilities for both red and blue. Results are obtained for a series of initial headings for the blue aircraft σ and are presented in polar form. The angular coordinate corresponds to the initial heading of blue; the radial coordinate is the survival probability. Red survival probability is shown as a solid line, blue survival is presented as a dashed line. For two initial headings a draw results. At $\sigma = 0$ both aircraft are initially in parallel flight to the north and a series of scissoring maneuvers are generated in MULTAC. Several high angle-off opportunities are recorded and a final survival probability of 45% is predicted for both aircraft. At $\sigma = 180$ deg where blue is initially heading south, the aircraft spiral around each other and by virtue of aircraft equality are unable to obtain shots. At positive headings blue has the angular advantage. His survival probability approaches 100% for even a moderate initial heading advantage; simultaneously red survival probability approaches zero for blue initial headings in the 30-90 deg range. For increasing values of σ red survival probability increases monotonically but always remains less than blue's until equality is reached in the region of the draw at $\sigma = 180$ deg. For negative values of σ the situation is reversed. Here red has the initial advantage and is able to tuck in behind blue where his survival probabilities approach 100%. Blue has a corresponding low survival probability.

Now consider the same series of encounters when blue is equipped with the advanced Phantom. Results are presented in Fig. 11. Now blue has an overwhelming advantage over most of the initial headings. The draw lines have moved to $\sigma = -45$ and -135 deg. The only red victories recorded are between these two initial blue headings. Even in this region red receives some fire and this survival probability peaks with a 75% value when blue is initially heading west away from red. The relative capability of these two aircraft in one-on-one encounters can be rapidly assessed by comparing the area of the initial blue heading/survival probability plane in which each dominates.

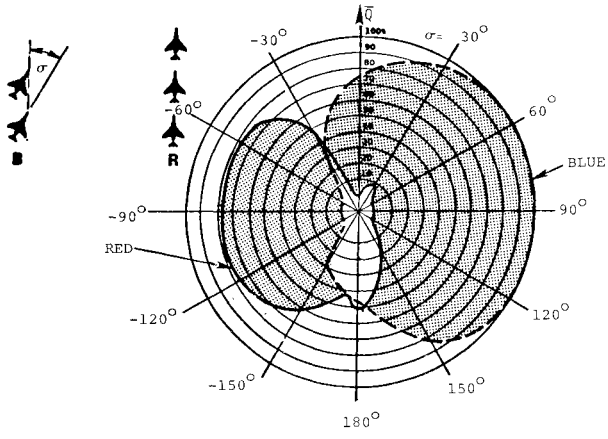

Fig. 13 Two-on-three survival probability, advanced blue aircraft.

Suppose now that one blue pilot flying the advanced aircraft encounters two red pilots flying standard F-4E aircraft. Thus we consider a situation where one side has an advanced technology aircraft and the other has deployed inferior performance aircraft but has a 2/1 numerical advantage. Figure 12 illustrates predicted survival probability for both forces over the heading range previously employed. In this set of encounters the draw lines are found at $\sigma = 60$ and 180 deg. Blue flying in the outnumbered high-technology aircraft is able to win the encounter only over a 120 deg range of initial headings. Red wins the remaining two-thirds of the encounters. Thus the numerically superior side flying inferior aircraft scores a decisive win in this situation.

Finally consider the case in which two blue pilots flying the advanced aircraft encounter three red pilots in the standard aircraft. Results are presented in Fig. 13. In this situation the overall advantage is seen to lie with the blue force even though it is outnumbered 3/2. It is clear from the results presented that technology can produce favorable results in aerial combat when equality of numbers is present or when modest numerical superiority lies with the opposing force. However, there is a limit to force size disadvantage which can be overcome by advanced technology alone. In the series of encounters considerd here a 25% increment in lift capability could offset a 3/2 numerical advantage but not a 2/1 disadvantage.

Conclusion

The recently developed MULTAC system has been outlined in some detail. Application of MULTAC has been illustrated by considering a set of M-on-N encounters in which advanced technology is traded against number of aircraft. In these examples it is clear that one-on-one results are not readily interpreted in an M-on-N context, for in this latter class of encounter force size ratio dominates the results. There are limits to the degree of numerical disadvantage which can be overcome by technology alone as demonstrated by the results presented. MULTAC provides the fighter designer and those concerned with addressing the issue of adequate force sizes with a rapid and low-cost investigative tool for the analysis of tradeoff problems in the air combat arena. It is in precisely this arena where performance capabilities of fighter aircraft are ultimately assessed.

Acknowledgment

This work was sponsored by the Air Force Flight Dynamics Laboratory, Contract F33615-78-C-3000.

References

[1] Hague, D.S., "An Introduction to Co-Kill Probability Estimation in the M-on-N Encounter," Paper 79-1729 presented at AIAA Guidance and Control Conference, Boulder, Col., Aug. 6-8, 1979.

[2] Merz, A.W. and Hague, D.S., "A Differential Game Solution to the Coplanar Tail-Chase Aerial Combat Problem," NASA CR-137809, Jan. 1976.

[3] Isaacs, R., *Differential Games*, John Wiley and Sons, New York, 1965.

[4] Hague, D.S. et al., "Combat Optimization and Analysis Program," Paper presented at Air to Air Combat Analysis and Simulation Symposium (U), AFFDL-TR-72-57, Vol. II, 1972.

[5] Bryson, A.E. and Denham, W.F., "A Steepest-Ascent Method for Solving Optimum Programming Problems," Raytheon Co., Missile and Space Div., Rept. BR-1303, 1961.

[6] Hague, D.S. and Glatt, C.R., "An Introduction to Multivariable Search Techniques for Parameter Optimization," NASA CR-73200, 1968.

[7] Wilde, D.J., *Optimum Seeking Methods*, Prentice-Hall, Englewoods Cliff, N.J., 1964.

[8] "U.S. Standard Atmosphere, 1962," U.S. Government Printing Office, Washington, D.C., 1962.

[9] Hague, D.S. et al., "Combat Optimization and Analysis Program," AFFDL-TR-71-52, May 1971.

[10] "F-4E Performance Data and Substantiation," McDonnell Aircraft Corp., Rept. F696, Aug. 1967.

[11] Axelson, J.A., "AEROX Computer Program for Transonic Aircraft Aerodynamics to High Angles of Attack," NASA TM X-73208, Feb. 1977.

[12] Hague, D.S., "Heuristic Approach to the Development of Ratings and Tactics Applicable to the One-on-One Combat Encounter," NASA CR-152000, July 1973.

[13] VonNeumann, J. and Morgenstern, O., *Theory of Games and Economic Behavior*, John Wiley & Sons, New York, 1943.